INTERNATIONAL JOURNAL OF
COASTAL & OFFSHORE ENGINEERING
IJCOE No. 4 / Autumn 2016 (19-25)

Oscillating Motion of Triangular Cylinder in a Viscous Fluid

Hamid Malah[1], Yuri Sergeyevich Chumakov[2], Sara Ramzani Movafagh[3]

[1]Department of Hydroaerodynamics, Institute of Applied Mathematics and Mechanics, Peter the Great St.Petersburg Polytechnic University, St. Petersburg, 194064, Russia; hamid.malah@gmail.com
[2]Department of Hydroaerodynamics, Institute of Applied Mathematics and Mechanics, Peter the Great St.Petersburg Polytechnic University, St. Petersburg, 194064, Russia; chymakov@yahoo.com
[3]Department of Civil Engineering and Applied Ecology, Institute of Civil Engineering, Peter the Great St.Petersburg Polytechnic University, St. Petersburg, 194064, Russia; sara.rm84@yahoo.com

ARTICLE INFO

Article History:
Received: 30 Aug. 2016
Accepted: 15 Dec. 2016

Keywords:
Triangular cylinder
Harmonic oscillation
Movable internal mass
Numerical simulation
OpenFOAM
Viscous fluid.

ABSTRACT

The system consisting of two rigid bodies in a viscous fluid is considered. The main body with mass M is placed in a viscous incompressible fluid, and the body with mass m moves inside the main body. This system is known as vibrobot which can be used in arbitrary inspection fluid mechanic objects such as oil industries pipes and tanks, as well as marine industries, medicine, etc. In this paper, the interaction between the vibrobot and viscous fluid is studied to achieve the motion laws of the vibrobot with the harmonic oscillation of internal mass. Also the flow structure around vibrobot and its effects on the hydrodynamic force acting on the vibrobot are investigated. Analyses are carried out by direct numerical simulation of the vibrobot motion in a viscous fluid by OpenFOAM package. Calculations are performed for the following combinations of control parameters; The ratio of the viscous fluid mass to the vibrobot mass $\mu_1=0.35$, the ratio of the internal mass to the vibrobot mass $\mu_2=0.325$ and dimensionless oscillation frequency f=1/5, when Reynolds number takes values in the range of $50<Re<250$. Calculations have been performed with different initial approximations, determined by different initial velocities of the incident flow.

1. Introduction

In this paper, numerical simulation of two-dimensional flow around a triangular cylinder subjected to a horizontal oscillating motion is considered in a viscous incompressible fluid. First of all, the history of studying bluff-body subjected to the fluid is expressed.

The liquid flow through a horizontal channel is a classical problem in the field of fluid mechanics. There are many cases where obstacles are in the path of fluid flows. When the flow separation due to an obstacle is very large, the obstacle may be classified as a bluff-body [1].

While a bluff-body in the fluid oscillates, or the body is fixed in the oscillating fluid, circulation around the body will be formed. Flow field around the bluff-body is usually divided into two main regions, i.e., an inner boundary layer and an outer flow field [2]. The study of two-dimensional oscillatory flow is important in the case of wave-induced forces on cylindrical structures and is the first step to understanding the complex three-dimensional structure of the wave. The flow due to loading and vibration of the cylinder in the viscous flow have been investigated during the recent decades [3].

A large number of numerical and experimental investigations on flow past variously shaped bodies have been accomplished by many researchers [4–8]. In contrast to the studies of the flow past a circular, square and rectangular cylinder, there are limited studies that focus on a triangular cylinder [9].

Wang et al. [10] experimentally presented a self-excited rotational oscillation on isolated and tandem triangular cylinders. Tatsuno [11] experimentally investigated the sample flow in the stable inner boundary layer near the triangular cylinder. In Tatsuno's paper, an equilateral triangular cylinder is used as a test body and oscillated sinusoidally in the fluid.

Numerical simulation of two-dimensional flow around a triangular cylinder subjected to a vertical oscillating motion in the channel were performed by Alawadhi [12]. In works of Jiahuang Tu et al. [13] the problem of two-dimensional fluid flow has studied numerically past the permanent and rotationally oscillating equilateral triangular cylinder with variable angle of

the incident, the Reynolds number, oscillating amplitude and oscillating frequency. Since the size of vibrobot is small, the Reynolds number is low. Therefore, flow around vibrobot is in the undetectable turbulence mode [14]. Thus, this problem is modeled as well as laminar mode. This principle can be used in medicine, arbitrary inspection fluid mechanic objects [15], etc.

Although many papers have been published on the flow around the different cylinders, lack of comprehensive study of triangular cylinders compared to round or square cylinders is obvious. Therefore, in this paper, a numerical simulation of the motion of the vibrobot in a viscous fluid is carried out by the OpenFOAM package with a simple harmonic oscillation on the triangular cylinder.

In this paper, a simplified plane setup of flow field and rigid body is assumed, that is symmetrical about the horizontal axis. The viscous and incompressible fluid is directed horizontally and the rigid triangular-shaped object (presenting one corner to the approaching flow and having one edge in the wake region) is allowed to move horizontally only. The main rigid body experiences (a) an inertia force due to the presence of a prescribed harmonic acceleration of a second internal mass, and (b) a horizontal force due to the presence of an outer fluid field with a certain coupling interface stress state. The central aim of the research presented in the paper is the characterisation and quantification of the induced fluid forces in order to determine the resulting locomotion of the object.

Geometrical Arrangement and Mathematical Equations

This section describes the model used for the rigid object and the surrounding flow. As the single degree of freedom of the object depends on the prescribed motion of the internal mass and the produced outer flow field, the solution of the Navier-Stokes equations is proposed in a moving coordinate system.

The system consisting of two rigid bodies in a viscous fluid is considered. The main body with mass M (corpus) is placed in a viscous incompressible fluid, and the body with mass m (internal mass) moves inside the main body. The triangular obstacle is in the middle of the considered zone. The dimensions of this zone are selected in a way which reduce boundary effects and satisfy the free-stream boundary condition and conform with other studies. The ratio of the vertical line of obstacle to the height of the channel is denoted by f which is called blockage ratio. To examine the effects of boundaries near obstacle on the characteristics of flow, $f = 0.033$ is reported as an acceptable value in many studies [1,2].

The internal mass interacts with the main body by a force which is generated by the actuator. The applied force to the internal mass, causes reaction force which effects to the main body. Reaction force changes the speed of the main body relative to the environment, hence resistance force of fluid changes in the opposite direction of the main body motion. Thus, adjusting the motion of the internal mass relative to the main body changes the external force acting on the main body in order to controlling the motion of the entire system. It is assumed that the internal mass has periodic longitudinal motion relative to the corpus which the entire system moves as a single assembly. Here, u_M is denoted as the velocity of the corpus, s and $z = \dot{s}$ are the motion and speed of the internal mass relative to the corpus, respectively that have been shown in Figure 1.

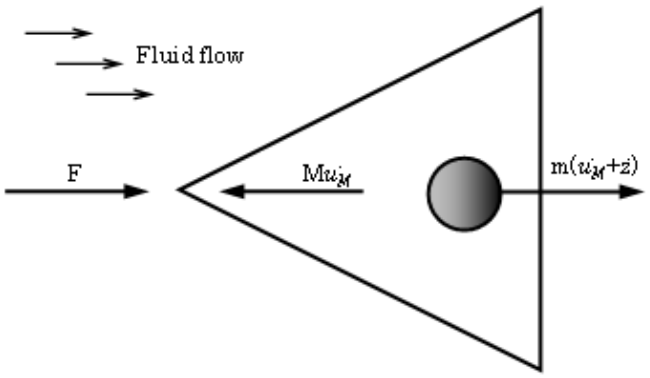

Figure 1: Schematic of the motion.

The equations of motion of the internal mass and corpus in a fixed coordinate system have the following form:

$$m(\dot{u}_M + \dot{z}) = -G \quad (1)$$

$$M\dot{u}_M = G + F \quad (2)$$

Here F is the horizontal force which is caused by the interaction between oscillating body and incident flow, G is the interaction force between the internal mass and corpus. By eliminating force G from equations (1) and (2), normalizing the speed by U_0 (velocity amplitude of the internal mass oscillations), normalizing the time by $RU_0{}^{-1}$ (R is the characteristic size of the corpus) and at last normalizing the force by $\rho_f RU_0{}^2$, the basic equation of entire system motion is obtained in the following form:

$$\dot{u}_M = -\mu_2\dot{z} + \mu_1(R^2/S)F \quad (3)$$

Here μ_2 is the ratio of the internal mass (moving mass) to the vibrobot mass ($\mu_2 = m/M + m$), μ_1 is the ratio of the viscous fluid mass (which occupies the same volume as the vibrobot) to the vibrobot mass ($\mu_1 = M_f/M + m$) and S is the cross sectional area of the corpus. Force F is determined by considering the motion of the fluid which surrounds the vibrobot.

The considered model is described by the non-steady Navier-Stokes system of equations. By normalizing the spatial coordinates, time and speed by R, $RU_0{}^{-1}$

and U_0 , respectively, vector form of the governing system of equations is as follows:

$$\partial U/\partial t + U.\nabla U = -\nabla p + \Delta U/Re \qquad (4)$$
$$\nabla.U = 0$$

Where $U = (u, v)$ is the dimensionless velocity, p is the dimensionless pressure and Re is Reynolds number. To solve this system of equations numerically, it is convenient to use the moving coordinate system associated with the vibrobot. To maintain the fluid motion in the form of a new non-inertial coordinate system, pressure should be defined as:

$$p = \tilde{p} + x\dot{\omega} \qquad (5)$$

Here the first term $\tilde{p}$ is the pressure in the fixed coordinate system, the second term $x\dot{\omega}$ is the contribution of the inertial components, $\dot{\omega}$ is the acceleration of the moving coordinate system and x is the dimensionless coordinate.
In the new coordinate system, on the boundary of the vibrobot, non-slip conditions (sticky fluid conditions) are defined:

$$u|_c = v|_c = 0 \qquad (6)$$

Where $u|_c$ is tangential velocity on the shell of triangular cylinder and $v|_c$ is normal velocity on the shell of triangular cylinder.
To determine the conditions at infinity, in this case, the acceleration of the moving coordinate system is written. For this purpose, the coordinate system should be switched to the moving coordinate system associated with the vibrobot. Hence the acceleration of the fixed coordinate system equals to the acceleration of the moving coordinate system plus acceleration of the coordinate system:

$$\dot{u}_M = \dot{\omega} + \dot{u}|_c \qquad (7)$$

Since $\dot{u}|_c = 0$, so

$$\dot{\omega} = -\mu_2\dot{z} + \mu_1(R^2/S)F \qquad (8)$$

At infinity, due to the fact that flow is potential, the boundary conditions are defined as follows:

$$\dot{u}|_\infty + \dot{\omega} = 0;\ \dot{u}|_\infty = -\dot{\omega} \qquad (9)$$

$$\dot{u}|_\infty = \mu_2\dot{z} - \mu_1(R^2/S)F \qquad (10)$$

With the assumption of potential flow at infinity, the condition of pressure can be obtained:

$$\partial p/\partial x\,|_\infty = -\dot{u}|_\infty = -\mu_2\dot{z} + \mu_1(R^2/S)F \qquad (11)$$

Calculated forces acting on vibrobot caused by viscous fluid in the dimensionless formulation are conducted by the following equation:

$$F_p = \int_S pnds - \int_S \bar{\sigma}.nds \qquad (12)$$

Where $\bar{\sigma}$ is the tensor of viscous stress, S is the vibrobot cross-sectional area and n is the outward normal vector to the vibrobot surface.
Thus, the obtained force vector F_p can be decomposed into the vertical component lift force F_y, and horizontal force F_x which consists of viscous resistance and inertial forces [3]. Inertial components are caused by acceleration of the fluid and consist of two parts; inertial added mass forces due to local acceleration near the cylinder and the Froude-Krylov forces, which is related with pressure gradient created in fluid which is used to simulate oscillating flow. In this case, Froude-Krylov forces can be calculated as:

$$F_{fk} = \int_S x\dot{\omega}\, nds \qquad (13)$$

Taking into account equation (13), the force F, acting on vibrobot in the moving coordinate system is calculated as:

$$F = F_x - F_{fk} \qquad (14)$$

Hence, the condition of pressure at infinity (equation (11)) can be rewritten as:

$$\partial p/\partial x\,|_\infty = -\dot{u}|_\infty = -\mu_2\dot{z} + \mu_1(R^2/S)(F_x - F_{fk}) \qquad (15)$$

The system of equations (4), (14) and (15) completely describe the motion of the vibrobot of any form in viscous fluid (and motion fluid around vibrobot) for a given motion law of the internal mass.
In the next step, the motion of a vibrobot with equilateral triangular cross-section is investigated in viscous fluid under harmonic oscillations of the internal mass:

$$\dot{z} = \sin(2\pi ft) \qquad (16)$$

Where $f = 1/KC$ is the dimensionless oscillation frequency. Here KC is Keulegan-Carpenter number [4].

Numerical solution

Discretization

This section describes the steps taken in order to solve the Navier-Stokes equations using an open-source framework (OpenFOAM).
Discretization of the computational domain is one of the solution processes [5]. In this work, block-structured grids is used which is built by a module in OpenFOAM known as blockMesh [6]. In Figure 2 a method for dividing the computational domain is presented.

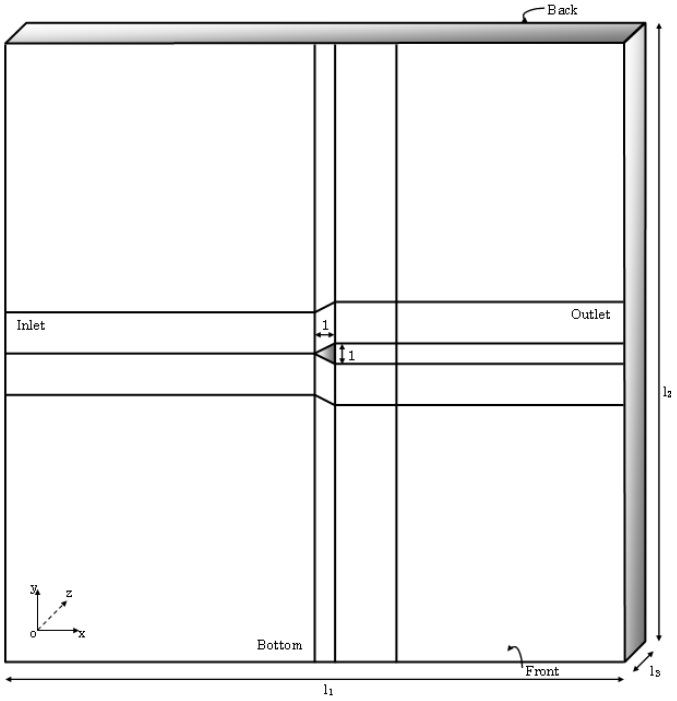

Figure 2: Division of the computational domain into blocks.

Here for two-dimensional calculations a domain with dimensions of $30 \times 30 \times 1$ is used where these values respectively point to length, height and width of the domain.

In Table 1 the values of the main parameters of the grids is presented. In Table 1; n is the total number of cells, N_m is the number of cells on the boundary of the cylinder, V_m is the volume of the smallest cells where is located in the boundary of the cylinder and V_{max} is the volume of the smallest cells where is located on the vicinity of the outer boundary of the domain. Additionally, in this table extremum values of indicators skewness M_s, non-orthogonality M_n and uniformity M_u for utilized grids, which are determined in accordance with the documentation of OpenFOAM package, are presented.

Table 1: Parameters of the computational grids.

Parameters	n	N_m	V_m	V_{max}	M_n	M_s	M_u
m_1	27652	197	.24 exp.(-4)	0.22	30	0.37	0.46
m_2	56734	131	8 exp.(-4	0.5	30	0.37	0.46

In OpenFOAM package, discretization of motion equations process is carried out by the finite volume method (FVM) in the Cartesian coordinate system. For this purpose, discrete values of velocity components and discrete values of pressure are located in the center of cells [7].

To minimize the errors due to the first order approximation, the time step (τ) in all the calculations is chosen from the condition $C^{max} < 0.1$. Here, C^{max} is the maximum Courant number [8]. Courant number in the OpenFOAM package is determined by the formula:

$$C = (|U_P|\tau)/\delta \tag{17}$$

Where $|U_P|$ is the velocity modulus in the cell, δ is the cell size in the direction of the velocity.

Boundary conditions

At the input and the output boundaries of the domain non-reflecting boundary conditions are set as:

$$\begin{cases} u = u_\infty;\ \partial p/\partial x = -\dot{u}_\infty; & u_0 > 0 \\ \partial p/\partial x = 0;\ p = -\dot{u}_\infty x; & u_0 \le 0 \end{cases} \qquad v = 0 \tag{18}$$

They are combined with the conditions of equation (15) which are defined on the boundary at infinity. Conditions depend on variable u_0, which defines flow direction relative to the outward normal vector at the boundaries.

At the top and the bottom boundaries non-slip conditions are laid down:

$$\partial p/\partial y = 0;\ \partial u/\partial y = 0;\ v = 0 \tag{19}$$

At the boundary of the cylinder non-slip conditions for the velocity are set:

$$u = v = 0 \tag{20}$$

The condition of pressure is:

$$\partial p/\partial n = 0 \tag{21}$$

At the front and the back boundaries of the domain special *"empty"* boundary conditions are given which are provided in OpenFOAM package in the case of non-responding calculations in an arbitrarily given direction. Required initial conditions in the entire computational domain, utilize the values of velocity and pressure corresponding to the undisturbed flow.

Verification

Due to lack of insufficient quantifications from the numerical solutions of triangular cylinders, and assuming that OpenFOAM is a mature solver, here in Figure 3, the flow pattern obtained by calculations in the OpenFOAM package is compared with the experimental results reported by Tatsuno [9]. In Tatsuno's study, glass micro-particles were suspended in a fluid to visualize the fluid flow and he also noted that $\vartheta = 0.53\ [cm^2/\mathrm{s}]$, that ϑ is kinematic viscosity. The results show that the entire structure of the flow obtained from the calculations and from the experiment are symmetrical about the axis of oscillation and as already seen, these flow patterns coincide qualitatively with each other.

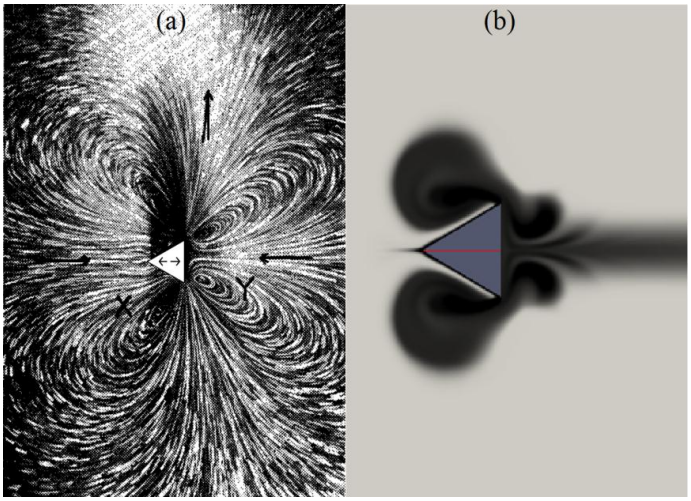

Figure 3: Flow pattern of a triangular cylinder in viscous fluid for $\upsilon = 0.53\ [cm^2/s]$. a) Experimental result reported by Tatsuno, b) Numerical solution using OpenFOAM package in this paper.

Results and Discussion

This section presents the results on the locomotion in a flow at small Reynolds numbers. Calculations have been performed for the following combinations of control parameters: $\mu_1 = 0.35$, $\mu_2 = 0.325$, and $f = 1/5$, in the range of $50 < Re < 250$. Results of calculations have been obtained with different initial approximations, determined by different initial velocities of the incident flow.

In the studied range, three stable modes of vibrobot motion were found. To describe these modes it is convenient to introduce the following motion characteristics: U_{ave} is the average speed of motion and η is the performance indicator of motion, describing the energy consumption of the body motion caused by internal motion. They are defined by the following equation:

$$\eta = N_0/N_{vbr}\ \% \qquad (22)$$

Here N_0 is the minimum power required to move the body with speed U_{ave} (values N_0 for different Re obtained according auxiliary calculations), N_{vbr} is the consumed power to move the vibrobot with speed U_{ave}.

Changes in characteristics of vibrobot motion with increasing Reynolds number for different modes of motion are shown in Figure 4 and Figure 5. In the zone of low Reynolds numbers ($Re < 160$) unique periodic symmetry was observed about the axis of oscillation (regime S), which determines the direction of motion of the vibrobot toward the positive direction of the x-axis. Increasing Reynolds number leads to increase in the average values of both speed and performance indicator of the vibrobot motion.

For range of Reynolds number greater than 180 two new regimes arise; for $180 < Re < 210$ quasi-periodic regime K_1 when $\vartheta = 48\ [cm^2/s]$ is observed and for $Re > 210$ quasi-periodic regime K_2 when $\vartheta = 46\ [cm^2/s]$ is observed.

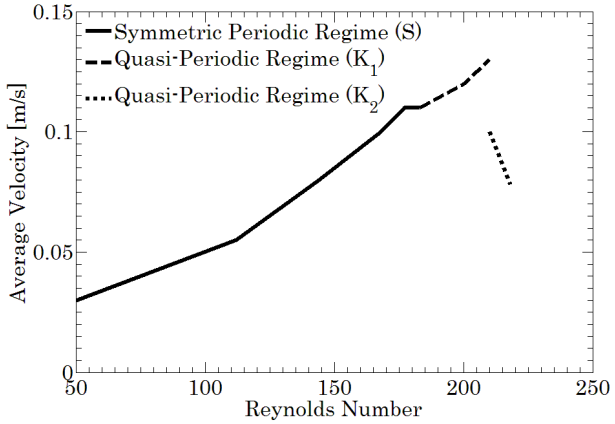

Figure 4: Motion characteristics of vibrobot; Dependence of average velocity on Reynolds number.

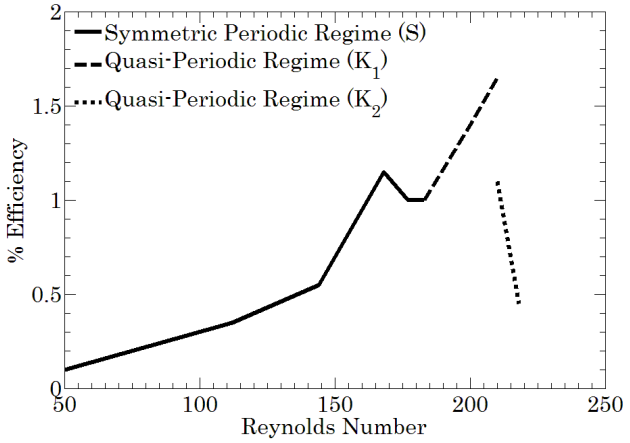

Figure 5: Motion characteristics of vibrobot; Dependence of efficiency on Reynolds number.

Moreover, in Figure 6, the flow patterns of different quasi-periodic modes are shown for a half period. Also schematic of velocity amplitude of the vibrobot versus time for regime K_1 when $\vartheta = 48\ [cm^2/s]$ is displayed in Figure7.

In Figure 8, velocity amplitude of the vibrobot versus time for two different modes with different initial conditions are shown. These modes are obtained for regime K_2 when $\vartheta = 46\ [cm^2/s]$. It is obvious that with different initial conditions, final velocity amplitudes are the same.

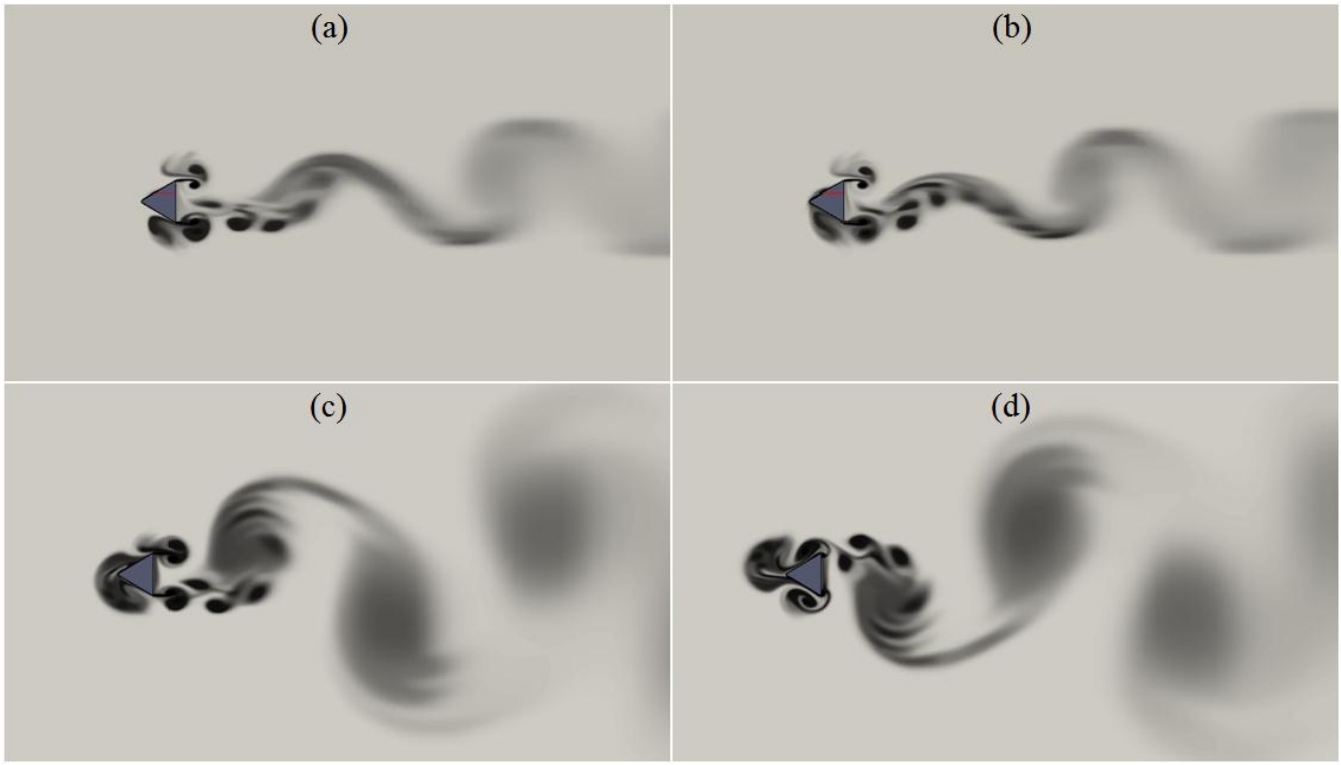

Figure 6: Flow pattern of a triangular cylinder in viscous fluid for a half period quasi-periodic modes. (a,b): Regime K_2 when $\upsilon = 46\ [cm^2/s]$ (c,d): Regime K_1 when $\upsilon = 48\ [cm^2/s]$.

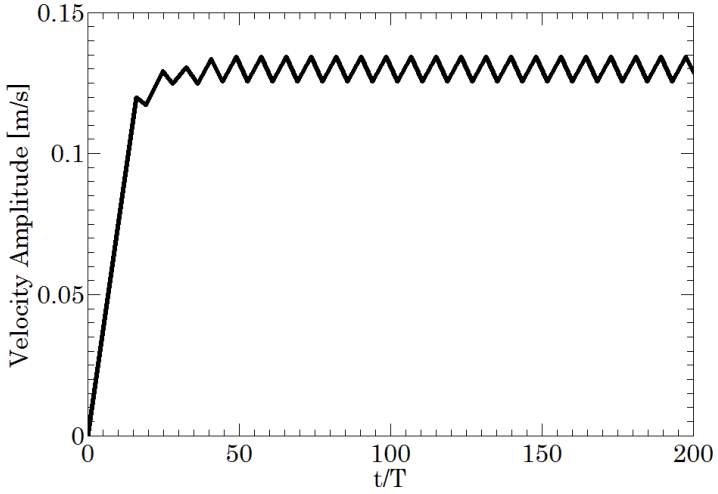

Figure 7: Velocity amplitude of the vibrobot versus time for regime K_1 when $\upsilon = 48\ [cm^2/s]$.

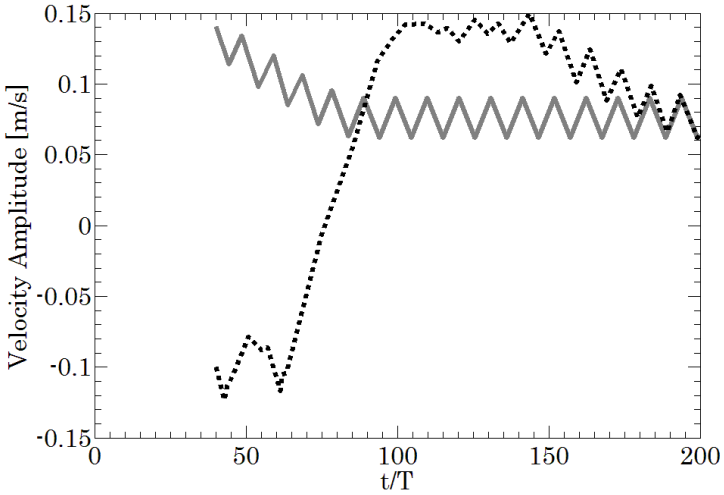

Figure 8: Velocity amplitude of the vibrobot versus time for two different initial conditions for regime K_2 when $\upsilon = 46\ [cm^2/s]$.

Summary and conclusions

In this paper, a triangular cylinder in a viscous fluid is considered which is under harmonic oscillations of the internal mass. The following results have been obtained:

1. The selected form for body under a given motion law of the internal mass for $f = 1/5$ (investigated oscillation frequency) allows to provide conditions for directional steady motion in a viscous fluid in the range of $50 < Re < 250$.

2. The direction of motion in most of the studied range is determined by the initial conditions, which by using that, different steady modes of straight motion of vibrobot can be realized, both in the positive direction of the x-axis and toward the negative direction of the x-axis but they have different effects.

3. Most of the observed flow regimes belong to the category of quasi-periodic modes, i.e. the full period of the vibrobot is equal to several periods of oscillation of the internal mass. Basic periodic flow regime turns into quasi-periodic flow regime at $Re > 180$. This is primarily due to the fact that with increasing Reynolds number, hydrodynamic force distinct the temporal harmonic oscillation from the main harmonic oscillation.

4. Maximum efficiency of motion, for the given parameters, does not exceed 1.7%. This value is achieved for the quasi-periodic regime K_1 for $Re = 210$. At high Reynolds numbers, less efficient modes have been observed, which gradually turn into chaotic.

All these results provide a basis for understanding the interaction between vibrobot and viscous fluid and it is a platform for studying more complex laws of motion in order to maximize the effectiveness of such devices.

References

[1] Abbassi, H., Turki, S., and Ben Nasrallah, S., ‘‘Numerical investigation of forced convection in a plane channel with a built-in triangular prism,’’ Int. J. Therm. Sci., Vol. 40, pp. 649–658, 2001.

[2] Tatsuno, M., and Bearman, P. W., ‘‘A visual study of the flow around an oscillating circular cylinder at low Keulegan-Carpenter numbers and low Stokes numbers,’’ J. Fluid Mech., Vol. 211, pp. 157–182, 1990.

[3] Koopmann, G.H., ‘‘The vortex wakes of vibrating cylinders at low Reynolds numbers,’’ J. Fluid Mech., Vol. 28, pp. 501–512, 1967.

[4] Davis, R. W., and Moore, E.F., ‘‘A numerical study of vortex shedding from rectangles,’’ J. Fluid Mech., Vol. 116, pp. 475–506, 1982.

[5] Saha, A. K., Biswas, G., and Muralidhar, K., ‘‘Three-dimensional study of flow past a square cylinder at low Reynolds numbers,’’ Int. J. Heat Fluid Flow., Vol. 24, pp. 54–66, 2003.

[6] Srigrarom, S., and Koh, A. K. G., ‘‘Flow field of self-excited rotationally oscillating equilateral triangular cylinder,’’ J. Fluids Struct., Vol. 24, pp. 750–755, 2008.

[7] Williamson, K., ‘‘Sinusoidal flow relative to circular cylinders,’’ J. Fluid Mech., Vol. 155, pp. 141–174, 1985.

[8] Ghadimi, P., Djeddi, S.R., Oloumiyazdi, M.H., and Dashtimanesh, A., ‘‘Simulation of flow over a confined square cylinder and optimal passive control of vortex shedding using a detached splitter plate,’’ Scientia Iranica transaction B- Mech. Eng., Vol. 22, pp.175–186, 2015.

[9] Alonso, G., Sanz-Lobera, A., and Meseguer, J., ‘‘Hysteresis phenomena in transverse galloping of triangular cross-section bodies,’’ J. Fluids Struct., Vol. 33, pp. 243–251, 2012.

[10] Wang, S., Zhu, L., Zhang, X., and He, G., ‘‘Flow Past Two Freely Rotatable Triangular Cylinders in Tandem Arrangement,’’ J. Fluids Eng., Vol. 133, 081202, 2011.

[11] Tatsuno, M., ‘‘Circulatory streaming in the vicinity of an oscillating triangular cylinder,’’ J. Phys. Soc. Japan., Vol. 38, pp. 257–264, 1975.

[12] Alawadhi, E. M., ‘‘Numerical Simulation of Fluid Flow Past an Oscillating Triangular Cylinder in a Channel,’’ J. Fluids Eng., Vol. 135, 041202, 2013

[13] Tu, J., Zhou, D., Bao, Y., Han, Z., and Li, R., ‘‘Flow characteristics and flow-induced forces of a stationary and rotating triangular cylinder with different incidence angles at low Reynolds numbers,’’ J. Fluids Struct., Vol. 45, pp. 107–123, 2014.

[14] Hémon, P., and Santi, F., ‘‘On the Aeroelastic Behaviour of Rectangular Cylindres in Cross-Flow,’’ J. Fluids Struct., Vol. 16, pp. 855–889, 2002.

[15] De, A. K., and Dalal, A., ‘‘Numerical simulation of unconfined flow past a triangular cylinder,’’ Int. J. Numer. Methods Fluids., Vol. 52, pp. 801–821, 2006.

[16] Morison, J. R., Johnson, J. W., and Schaaf, S. A., ‘‘The Force Exerted by Surface Waves on Piles,’’ J. Pet. Technol., Vol. 189, pp. 149–154, 1950.

[17] Justesen, P., ‘‘A numerical study of oscillating flow around a circular cylinder,’’ J. Fluid Mech., Vol. 222, pp. 157–196, 1991.

[18] Issa, R. I., ‘‘Solution of the implicitly discretised fluid flow equations by operator-splitting,’’ J. Comput. Phys., Vol. 62, pp. 40–65, 1986.

[19] Versteeg, H. K., and Malalasekera, W., *An introduction to computational fluid dynamics: the finite volume method*, Longman, 2007.

[20] Shademani, R., Ghadimi, P., Zamanian, R., and Dashtimanesh, A., ‘‘Assessment of Air Flow over an Equilateral Triangular Obstacle in a Horizontal Channel Using FVM,’’ J. Math. Sci. Appl., Vol. 1, pp. 12–16, 2013.

[21] Ferziger, J. H., and Peric, M., *Computational Methods for Fluid Dynamics*, Springer, 2002.